

# Small Scale Yielding Model for Fracture Mechanics

J. Thomas, K. C. Koppenhoefer\*, J. S. Crompton

AltaSim Technologies, LLC

\*Corresponding author: 130 East Wilson Bridge Road, Suite 140, Columbus, OH 43085, USA

Kyle@AltaSimTechnologies.com

**Abstract:** The small scale yielding model is used to compare published linear elastic fracture mechanics (LEFM) and elastic-plastic fracture mechanics (EPFM) analytical solutions to elastic and plastic finite-element solutions developed using COMSOL Multiphysics. The EPFM solutions include small-strain and large-strain solutions. In addition, these cases are also developed using Abaqus as a point of comparison. This work compares and contrasts the solution methodology and results of COMSOL Multiphysics with finite element analysis software with an extensive history of solving fracture mechanics problems.

**Keywords:** fracture mechanics, crack, small-scale yielding model, small-strain plasticity, large-strain plasticity.

## 1. Introduction

Materials that experience cleavage fracture due to pre-existing cracks fail due to the elevated stress ahead of these cracks. Conventional fracture mechanics has developed single parameters that seek to uniquely describe the displacement, strain and stress ahead of a crack. For materials that do not undergo plastic deformation, the single parameter is referred to as  $K$ . When plastic strain develops at the crack tip, the  $J$ -integral provides this single parameter. If plasticity remains well contained to the crack tip region and is not influenced by the size of the surrounding structure, then  $K$  and  $J$  are uniquely related such that

$$K = \sqrt{\frac{EJ}{1 - \nu^2}} \quad (1)$$

where  $E$  is the elastic modulus and  $\nu$  is Poisson's ratio. This condition is referred to as Small Scale Yielding (SSY) since the plastic zone is small in comparison to the relative dimensions of the structure in which it is contained. As material toughness increases, the plastic zone at the crack tip increases in size and

eventually interacts with the finite boundaries of the structure in which it is contained thus exceeding the SSY condition.

To examine the effects of violating SSY conditions on the displacement, strain and stress in structures, much research in the field of fracture mechanics relies on computational modeling. The COMSOL Multiphysics Model Gallery gives a model of an edge crack [1] where calculated stress intensity factors are compared with the classic, single parameter linear elastic fracture mechanics (LEFM) solution developed by Irwin [2]. This model gives confidence in COMSOL Multiphysics ability to accurately predict cleavage fracture in brittle materials where fracture toughness is low and SSY conditions are met. On the opposite extreme, limit load analysis is used to determine failure when fracture toughness is high and failure is governed by the plastic flow characteristics of the material.

Many structures are constructed using steels with moderate fracture toughness values that do not fit into either of these two extremes.

For this important class of problems, the field of non-linear fracture mechanics, specifically elastic-plastic fracture mechanics (EPFM), has developed equations and models for describing the displacement, strain and stress ahead of a crack where plasticity effects cannot be neglected [3]. EPFM relies upon SSY as an important benchmark. This SSY modeling assumption has given rise to a number of analytical solutions including that developed by Rice and Rosengren [4] and Hutchinson [5] known as the HRR singularity solution. Now, even the best published analytical stress results break down in a singular zone near the crack tip being based on small strain theory. For these areas, finite-element analysis with a large-strain theory that takes into account geometry changes due to crack blunting is more accurate.

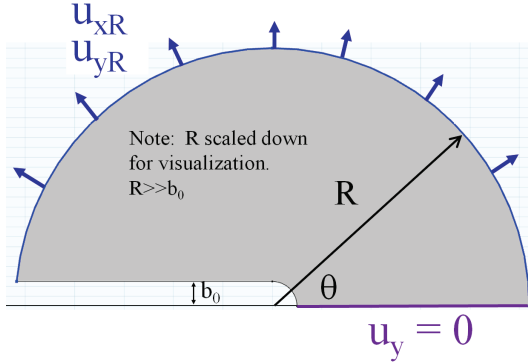


**Figure 1. Blunted crack with displacement boundary conditions. Initial radius of crack width,  $b_0=10\mu\text{m}$ . Specimen radius,  $R=150\mu\text{m}$ .**

## 2. COMSOL Model

### 2.1 Material Model

The analyses conducted in this work use three distinct material models available within COMSOL Multiphysics: linear elastic, small-strain plasticity, and large-strain plasticity. For the linear elastic model, a linear constitutive model and linear strain-displacement relationships are used.

$$\nabla \cdot \boldsymbol{\sigma} = \mathbf{F}\mathbf{v}, \quad (2)$$

$$\mathbf{S} = \mathbf{C} : \boldsymbol{\varepsilon} \quad (3)$$

$$\boldsymbol{\varepsilon} = \frac{1}{2} (\nabla \mathbf{u} + (\nabla \mathbf{u})^T) \quad (4)$$

For the small-strain plasticity model, the linear strain-displacement relationships are used as they were in the linear elastic model. (This decision is implemented by choosing to leave the “Geometric Non-linearity” option unchecked under the “Study Settings” section of the COMSOL Multiphysics Study Node.) The constitutive model is a Ramberg-Osgood power law plasticity model defined as

$$\frac{\boldsymbol{\varepsilon}}{\boldsymbol{\varepsilon}_0} = \frac{\boldsymbol{\sigma}}{\boldsymbol{\sigma}_0} + \alpha \left( \frac{\boldsymbol{\sigma}}{\boldsymbol{\sigma}_0} \right)^n \quad (5)$$

and implemented by a user-defined interpolation function to define the post-yield hardening behavior of the material. Table 1 provides the material property parameters.

**Table 1: Ramberg-Osgood Power-Law Material**

Parameter	Value	Unit
Young's modulus, E	200	GPa
Poisson's ratio, $\nu$	0.33	n/a
Yield strength, $\sigma_0$	250	MPa
Yield offset, $\alpha$	0.002	n/a
Power law exponent, n	13	n/a

Equation (5) gives the plastic flow rule for the small-strain case.

$$\mathbf{S} = \mathbf{C} : (\boldsymbol{\varepsilon} - \boldsymbol{\varepsilon}_p) \quad (6)$$

$$F(\boldsymbol{\sigma}, \boldsymbol{\sigma}_0) \leq 0, \quad (7)$$

$$\dot{\boldsymbol{\varepsilon}}_p = \lambda \frac{\partial Q}{\partial \boldsymbol{\sigma}} \quad (8)$$

The large-strain material model eliminates the assumption of small displacements in the strain-displacement relationship and uses the Ramberg-Osgood constitutive model specified in Eq. (5).

$$\boldsymbol{\sigma} = \mathbf{J}^{-1} \mathbf{F} \mathbf{S} \mathbf{F}^T, \quad (9)$$

$$\mathbf{F} = (\mathbf{I} + \nabla \mathbf{u}), \quad (10)$$

$$\begin{aligned} \mathbf{J} &= \det(\mathbf{F}) \\ \boldsymbol{\varepsilon} &= 1/2 [\nabla \mathbf{u} + (\nabla \mathbf{u})^T \\ &\quad + (\nabla \mathbf{u})^T \nabla \mathbf{u}] \end{aligned} \quad (11)$$

### 2.2 Crack Loading

Figure 1 gives a schematic of the blunted crack for the small scale yielding model.

The loading is applied using displacement conditions as a crack tip displacement field for Mode I:

$$\begin{aligned} u_{xR} &= \frac{K}{2G} \sqrt{\frac{r}{2\pi}} \cos\left(\frac{\theta}{2}\right) \left[ \kappa - 1 + 2 \sin^2\left(\frac{\theta}{2}\right) \right] \\ u_{yR} &= \frac{K}{2G} \sqrt{\frac{r}{2\pi}} \sin\left(\frac{\theta}{2}\right) \left[ \kappa + 1 - 2 \cos^2\left(\frac{\theta}{2}\right) \right] \end{aligned} \quad (12)$$

where

$$\kappa = 3 - 4\nu \quad (\text{plane strain})$$

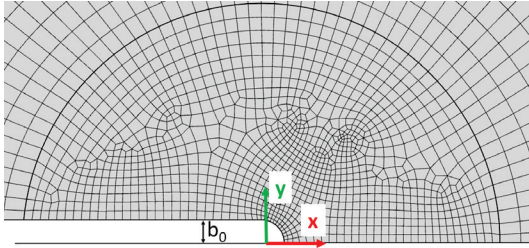


**Figure 2. 2D half symmetric small scale yielding model. Initial crack width,  $b_0=10\mu\text{m}$ . A quad mesh is generated; isoparametric elements with quadratic shape order discretization are specified.**

### 2.3 Meshing and Discretization

A free quad mesh (with custom size constraints) generates the mesh in the region near the crack tip. The mapped meshing functionality provides a more efficient mesh in the remaining regular shaped arcs (see Figure 2).

A quadratic discretization was used for both the solution shape order and geometry shape order (isoparametric elements). For the solid mechanics elements, COMSOL Multiphysics does not give the freedom for the user to control how to perform the element integration. The software constrains the integration order to twice the order selected for the shape functions, and this constraint could introduce locking.

### 2.4 J-integral Calculations

The J-integral is given by:

$$J = \frac{K^2}{E} = \int_{\Gamma} W_s dy - T_i \frac{\partial u_i}{\partial x} ds \quad (13)$$

$$= \int_{\Gamma} \left( W_s n_x - T_i \frac{\partial u_i}{\partial x} \right) ds$$

where

$$W_s = \frac{1}{2} (\sigma_x \varepsilon_x + \sigma_y \varepsilon_y + 2\sigma_{xy} \varepsilon_{xy})$$

is strain energy density

$$T_x = \sigma_x n_x + \sigma_{xy} n_y, \quad T_y = \sigma_{xy} n_x + \sigma_y n_y$$

are traction vector components

The J-integral calculation in COMSOL Multiphysics uses path lines that are in line with the coordinate directions (see Figure 3). For curved paths (green path), the J-integral calculation within COMSOL Multiphysics may be path-dependent due to the normal vector for the traction integral calculation not pointing outwards. To ensure that the contour normal are pointing outwards for all node points, the normal is specified explicitly rather than using the solid.nx and solid.ny path normal operators. These path normal operators cannot guarantee to be pointed outward causing some negative energy components to give a J-integral less than the actual J-integral.

### 2.5 Solution procedure

The non-linear stationary solver was used with the load ramping technique to aid in convergence. The default Newton non-linear method was selected but the damping settings were set to “Automatic highly nonlinear”. Total degrees of freedom equal approximately 60,000.

## 3. Results and Discussion

For comparison, the normal stress (normalized by yield strength) along the length of the remaining ligament is plotted using the line graph post-processing functionality. Also, the x-distance along the ligament is normalized by the yield strength divided by the J-integral loading rate. With this normalization, a value of 1 on the x-axis corresponds to approximately twice the crack tip opening displacement.

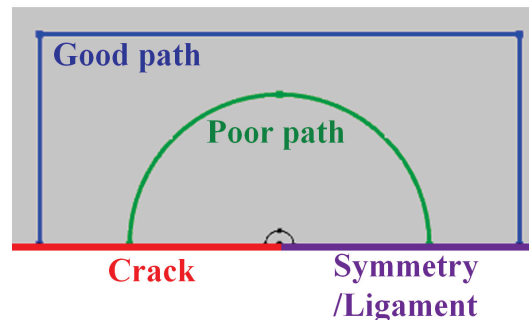


**Figure 3. 2D half symmetric small scale yielding model with 2 J-integral path definitions. The blue path works well because the lines are in the direction of the x and y coordinate directions.**

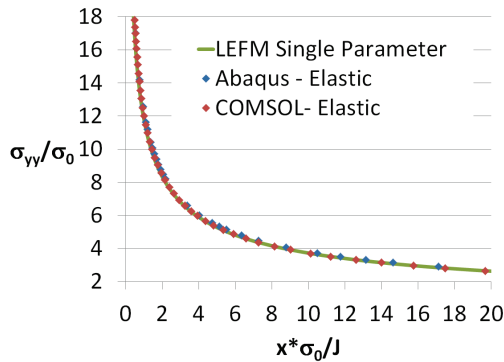


Figure 4. Normal stress on remaining ligament versus distance along ligament normalized by loading for linear elastic case.

Figure 4 gives the comparison between the LEFM single parameter Irwin solution along the ligament given by

$$\sigma_{yy} = \frac{K}{\sqrt{2\pi x}} \quad (14)$$

and the FEA predictions given by both COMSOL Multiphysics and Abaqus. The results show good agreement for all three methods.

Figure 5 gives the comparison between the HRR singularity solution based on EPFM theory given by

$$\sigma_{yy} = \sigma_0 \left( \frac{EJ}{\alpha \sigma_0^2 I_n x} \right)^{\frac{1}{n+1}} \tilde{\sigma}_{\theta\theta}(n, 0) \quad (15)$$

$$I_n = I_{13} = 4.4$$

$$\tilde{\sigma}_{\theta\theta}(13,0) = 2.6$$

and the FEA small strain formulation predictions given by both COMSOL Multiphysics and Abaqus. Both FEA software show good agreement. Additionally, the FEA results match the HRR solution reasonably well in the intermediate region less than about one crack tip radii away from the crack tip. The COMSOL Multiphysics results demonstrate an oscillatory response in the region near the crack tip likely due to locking due to the dilatational

contribution to the stiffness causing locking for near incompressible conditions.

Additionally, it is worth noting that the Gauss point evaluation for normal stress (i.e. solid.sGpy) rather than the “legacy” stress evaluation (i.e. solid.sy) must be used for accurate evaluation especially in the region near the crack tip. The Gauss point evaluation interpolates directly from the integration points which are the only place where the force balance equation is guaranteed to be satisfied for non-linear material models. In contrast, the less-accurate legacy evaluation interpolates from the Lagrange points (node points) and is an evaluation based on the derivative of the displacements at these points.

For the large plastic strain formulation, Figure 6 shows plastic strain contours (mirrored across the symmetry plane) near the crack tip for loading of  $K=22.1 \text{ MPa}\sqrt{\text{m}}$ . Results are compared to the plastic zone size estimate from LEFM as given by the following equation:

$$r_y(\theta) = \frac{1}{4\pi} \left( \frac{K}{\sigma_0} \right)^2 \left[ 1 + \cos\theta + \frac{3}{2} \sin^2\theta \right] \quad (16)$$

The LEFM solution for the radius of the plastic zone as a function of rotational angle specifies the location where the stress equals the yield stress of the material. The over prediction of the plastic zone size by the LEFM solution appears consistent with the over prediction of the stress ahead of the crack tip by the LEFM solution compared to the EPFM solution (see Figure 7).

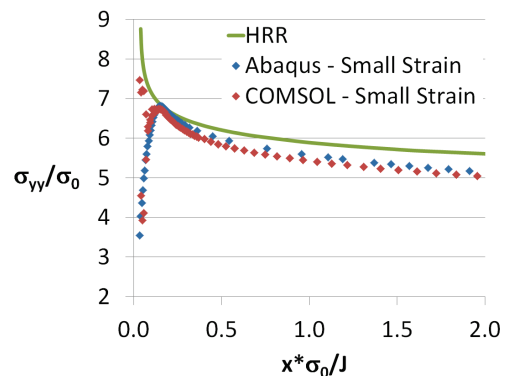


Figure 5 Normal stress on remaining ligament versus distance along ligament normalized by loading for elastoplastic small strain case. Notice the locking distorting the solution for the COMSOL Multiphysics case near the crack tip.

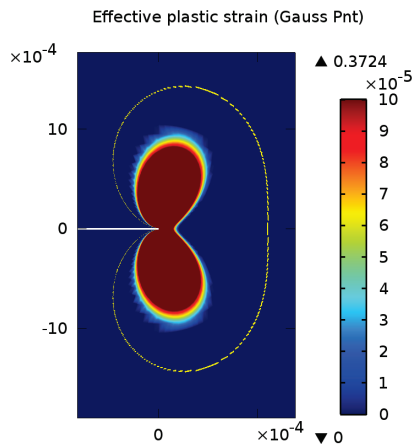


Figure 6. Plastic strain contour plot (COMSOL Multiphysics solution) for area near crack tip for loading,  $K=22.1 \text{ MPa}\sqrt{\text{m}}$ . Yellow line shows the plastic zone size estimate from LEFM (Eqn. 8).

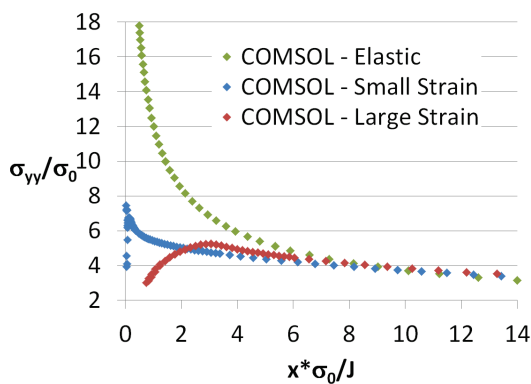


Figure 7. Normal stress on remaining ligament versus distance along ligament normalized by loading for LEFM, and EPFM (small and large strain formulations).

Figure 8 shows the quantitative comparison between COMSOL Multiphysics and Abaqus for the large-strain FEA predictions. Good agreement is seen between the two modeling software. The HRR singularity solution is given for reference, but as noted before the HRR solution breaks down near the crack tip due to the effects of crack tip blunting that occurs in EPFM.

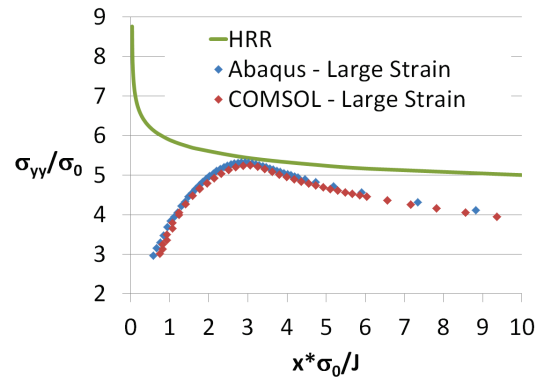


Figure 8. Normal stress on remaining ligament versus distance along ligament normalized by loading for elastoplastic large strain formulation. The FEA results are better than the HRR singularity assumption for the region near the crack tip.

Figure 9 shows how the Abaqus reduced integration formulation is much better than the Abaqus full integration formulation. From the extreme distortion seen in the Abaqus full integration results as compared to COMSOL Multiphysics, we postulate that COMSOL Multiphysics has some sort of reduced integration or other numerical scheme automatically implemented in their solid mechanics elements to mitigate locking. However, documentation is silent on this matter.

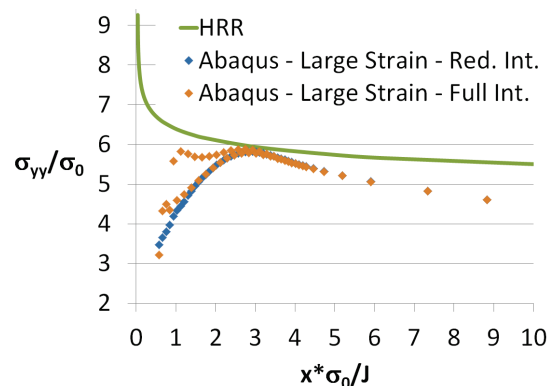


Figure 9. Normal stress on remaining ligament versus distance along ligament normalized by loading for Abaqus large strain formulation with reduced integration and with full integration. Full integration shows locking which distorts the results.

## 4. Conclusions

This study shows that COMSOL Multiphysics produces displacement, strain and stress results consistent with available analytical solutions and FEA solutions generated by Abaqus.

COMSOL Multiphysics could improve fracture mechanics modelling functionality by adding pre-defined J-integral calculations that are robust for general path definitions (notably curved paths). Also, COMSOL Multiphysics could include options for the integration order used with the solid mechanics elements.

Anyone wishing to duplicate these results should use the Gauss point evaluation of stresses and plastic strains (e.g. `solid.sGpy` and `solid.epeGp`). The legacy evaluation (e.g. `solid.sy` and `solid.epe`) produces oscillations in these variables for the large strain case.

## 5. References

1. COMSOL Multiphysics Model Gallery, Single Edge Crack, Model ID: 988
2. Irwin, G.R., Analysis of Stresses and Strains Near the End of a Crack Traversing a Plate, *Journal of Applied Mechanics*, **Volume 24**, 361-364 (1957)
3. Anderson, D.T., *Fracture Mechanics: Fundamentals and Applications*. CRC Press, Boca Raton (1991)
4. Rice, J.R. and Rosengren, G.F., Plane Strain Deformation Near a Crack Tip in a Power-Law Hardening Material, *Journal of the Mechanics and Physics of Solids*, **Volume 16**, 1-12 (1968)
5. Hutchinson, J.W., Singular Behavior at the End of a Tensile Crack Tip in a Hardening Material, *Journal of the Mechanics and Physics of Solids*, **Volume 16**, 13-31 (1968)